Available online at www.sciencedirect.com
SCIENCE DIRECT
ELSEVIER
Journal of the European Ceramic Society 26 (2006) 409–415
ECERS
www.elsevier.com/locate/jeurceramsoc

Formation and micro-Raman spectroscopic study of Aurivilius and fluorite-type $SrBi_2Nb_2O_9$ nanocrystallites obtained using an 'amorphous citrate' route

Daniel Nelis [a], José M. Calderon-Moreno [b,*], Mónica Popa [b], Marlies K. van Bael [a], J. Mullens [a], L.C. van Poucke [a]

[a] *Limburgs Universitair Centrum, Laboratorium voor anorganische en fysische scheikunde, Universitaire Campus Gebouw D, Diepenbeek 3590, Belgium*
[b] *Universitat Politécnica de Catalunya EPSC, Department of Applied Physics, Av. Canal Olimpic s/n, Castelldefels, 08860 Barcelona, Spain*

Available online 2 November 2005

Abstract

The crystallization of a $SrBi_2Nb_2O_9$ gel-glass obtained using the amorphous citrate method was studied by micro-Raman scattering, X-ray diffraction, and electron microscopy techniques. A citric acid–ethanolamine gel with the stoichiometric proportion of the metallic cations was prepared as polymeric precursor and calcined to obtain the amorphous complex. Nanocrystallites with a metastable fluorite-type structure nucleate from the amorphous complex below 500 °C, as shown by X-ray scattering and confirmed by electron microscopy. The morphological study by scanning electron microscopy revealed the nucleation of nanocrystals in the glass-like amorphous powder after thermal treatment at 500 °C. Raman features characteristic of the stable Aurivillius nanocrystals can be detected after thermal treatment at 550 °C, while using X-ray diffraction the crystallization of the Bi-layered perovskite phase is observed only after treatment at 625 °C or higher temperatures. Both X-ray and Raman scattering detected single phase nanocrystallites with Aurivillius structure above 650 °C. The distinctive Raman features of the different $SrBi_2Nb_2O_9$ nanocrystallites and its evolution with thermal treatment is presented.

Keyword: Powders-chemical preparation; Precursors-organic; Raman spectroscopy; $SrBi_2Nb_2O_9$ nanocrystallites

1. Introduction

$SrBi_2Nb_2O_9$ (SBN) is an $n = 2$ member of the Aurivillius family of layered perovskites. It is orthorhombic at room temperature, with a Curie temperature ~430 °C. SBN presents interest as lead-free high temperature piezoelectric with very high resistance to electrical fatigue during ferroelectric switching, i.e. for applications substituting PZT.

SBN ceramics are normally prepared by solid state methods,[1] but the loss of Bi at high temperature promotes the formation of an undesirable non-ferroelectric Bi-deficient pyrochlore phase.[2] Bulk powders can be prepared by low temperature methods, i.e. aqueous solution,[3] or combustion synthesis.[4] The preparation of SBN thin films has been reported both by 'chemical' methods, i.e. using an aqueous solution gel route,[5,6] or by sol–gel[7] and by 'physical' methods: pulsed laser ablation.[8] Advantages of a polymeric precursor water route include an excellent control of the stoichiometry, good structural homogeneity of nanocrystalline powders (i.e. control of particle size, absence of agglomerates) difficult to achieve by other low temperature methods, i.e. combustion synthesis; the use of simpler equipment and cheap reagents compared to physical methods and the use of moderate temperatures, thus avoiding the formation of the unwanted pyrochlore phase.

Compared to other Bi-layered perovskite oxides, such as $SrBi_2Ta_2O_9$ (SBT),[9,10] SBN offers the advantage of a lower preparation temperature. However, the nucleation process of SBN powders is not well known. The crystallization

* Corresponding author.
E-mail address: jose.calderon@upc.es (J.M. Calderon-Moreno).

0955-2219/$ – see front matter © 2005 Elsevier Ltd. All rights reserved.
doi:10.1016/j.jeurceramsoc.2005.07.049

of metastable phases with fluorite structure at low temperature has been reported, but there is no study on the experimental conditions, i.e. thermal treatment, particle size, which lead to the formation of the intermediate fluorite SBN.

The present study aims to investigate the crystallization from an amorphous complex with SBN stoichiometry of Bi-layered perovskite-type nanocrystallites of the Aurivillius phase via an intermediate fluorite-SBN phase. Raman scattering has been used prominently to determine the nucleation of the different phases. The different Raman features characteristic of each phase and its evolution with thermal treatment and microstructural changes are presented. The use of a Raman microprobe allows the local study of the nanocrystallites in the analyzed areas ($\sim 2\ \mu m^2$).

2. Experimental

2.1. Preparation of the Nb-precursor

The preparation of aqueous Nb-, Bi-, and Sr-precursors have been described previously.[11–15] Aqueous solution–gel synthesis of ceramics containing group Vb metals (like Nb in SBN) is very complicated since very few salts are water-soluble because of the high valency and the subsequent fast hydrolysis. Nevertheless, a stable aqueous Nb-precursor can be prepared starting from Nb-oxalate.[12] A peroxo-citrato-niobium(V) precursor solution is prepared by a synthesis route similar to that of Narendar et al.[13] Although Nb-oxalate is water-soluble, it is however not suitable for gel formation. The first synthesis step comprises the dissolution of niobium(V) ammonium oxalate in an aqueous solution of citric acid and hydrogen peroxide. After heating this mixture at 150 °C, a yellow precipitate of niobic acid is formed. After isolating it by filtration, this Nb-compound is used as Nb-source for synthesis.

2.2. Preparation of the Bi-precursor

An aqueous Bi-precursor is obtained by dissolution of Bi-citrate in water and ethanolamine.[14,15]

2.3. Preparation of the SBN-precursor

The three-metallic SBN-solution is prepared by the addition of Sr-acetate to a mixture of the Nb- and the Bi-precursor solutions in stoichiometric amounts. In order to obtain a stable solution, an excess of citric acid has to be added.

2.4. Thermal treatments

To induce the formation of SBN crystallites, we used thermal treatment at 550, 650, 700 and 750 °C for 2 h at a rate of 5 °C/min.

2.5. Powder X-ray diffraction

The crystalline structure and phase purity of the obtained samples were characterized the X-ray powder diffraction (XRD), using a Siemens D5000 diffractometer with Cu Kα radiation. The XRD patterns were collected with an angle step of 0.01 for all measurements.

2.6. Raman

Raman spectra of all the samples were recorded at room temperature on a Jobin Yvon T64000 Raman microspectrometer equipped with a triple monochromator and a coupled-charge device detector.

2.7. SEM

Samples were observed in an JEOL apparatus after Pt–Pd coating.

3. Results

X-ray diffraction. The evolution of XRD patterns after different thermal treatments is shown in Fig. 1. Patterns 1a and b, measured after thermal treatment up to 400 °C, clearly reveal the amorphous nature of the SBN precursor. The XRD patterns 1c and d, after treatment up to 600 °C, show characteristic peaks corresponding to the planes (1 1 1), (2 0 0), (2 2 0) and (3 1 1) of a SBN-fluorite phase. The patterns have broad diffraction peaks, attributed to a very small crystallite size of the SBN fluorite nanocrystallites. The crystallite size calculated using the Scherrer equation

$$L = \frac{0.9\lambda}{\beta \cos \theta}$$

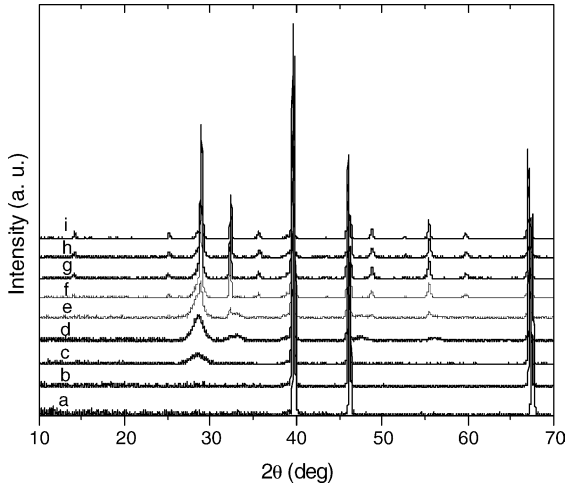

Fig. 1. XRD pattern after thermal treatment at 25 °C (a), 400 °C (b), 500 °C (c), 600 °C (d), 625 °C (e), 650 °C (f), 700 °C (g), 800 °C (h) and 900 °C (i).

where L is the mean crystallite size, β the full width at half maximum and λ the used wavelength (1.54183 Å), is about 6 nm. At 600 °C, we can observe the same broad features of SBN-fluorite than at 500 °C, although with more intense peaks.

At 625 °C a drastic change occurs, the XRD pattern in 1e reveals the formation of a new phase with the SBN Bi-layered perovskite structure, accompanied by a rapid growth of the particle size to mean values of ∼80 nm in the new crystallites, while crystallite sizes of SBN-fluorite nanocryustallites remain one order of magnitude smaller. At this temperature the XRD features of both phases coexist. The XRD pattern of the sample treated at 650 °C clearly reveals the formation of SBN-layered perovskite phase at the expense of SBN-fluorite. Only small traces of the fluorite features remain, and the layered perovskite is at large the main phase at 650 °C. The XRD patterns in 1g, h and i, above 700 °C, show only the features of Bi-layered perovskite SBN crystallites.

The XRD spectra indicates that SBN crystallites are already transformed into the 'Aurivillius' phase with double-perovskite structure at 650 °C. Only at 625 °C XRD features of both allotropes can be observed simultaneously.

3.1. Scanning electron microscopy (SEM)

SEM reveals an evident change in the sample treated at 500 °C (Fig. 2). The onset of crystallization, due to the nucleation of SBN-fluorite nanocrystallytes in the amorphous precursor below 500 °C, clearly modifies the appearance of the pellets from a typical gel-glass structure to that of polycrystalline pellets. Elemental analysis by EDX, Fig. 2, indicates that the proportions of the metal cations remained unchanged after nucleation of the SBN nanocrystallites and a significant reduction of the intensity in the C peak. The formation of elongated 'rodlike' nanocrystallites was observed by SEM after thermal treatment at 700 °C. The anysotropic shape of the rodlike nanocrystallites is caused by the differences in the growth rate for different crystalline planes during the growth of Bi-layered perovskite crystals, with a complex crystal sytructure.

3.2. Raman

In situ Raman microspectroscopy is an useful tool for studying the crystallization process from amorphous and determining the optimum conditions for thermal treatment. Vibrational spectroscopy studies were carried out to confirm the structural changes undergone by the amorphous precursor treated at different temperatures. The samples treated below 550 °C showed luminescence in the used experimental conditions. The observed luminescence is attributed to the presence of unburned organics, because the combustion of the organic part of the complex is not complete at this temperature.

After thermal treatment at 550 °C, luminescence effects disappear from the spectra, due to the complete combustion of the organic part of the amorphous complex. Amorphous carbon is a common impurity formed during the combustion of the organic part in samples prepared from an amorphous metal-complex route, especially when the complex has an elevated C content. It is not normally detected by XRD but it

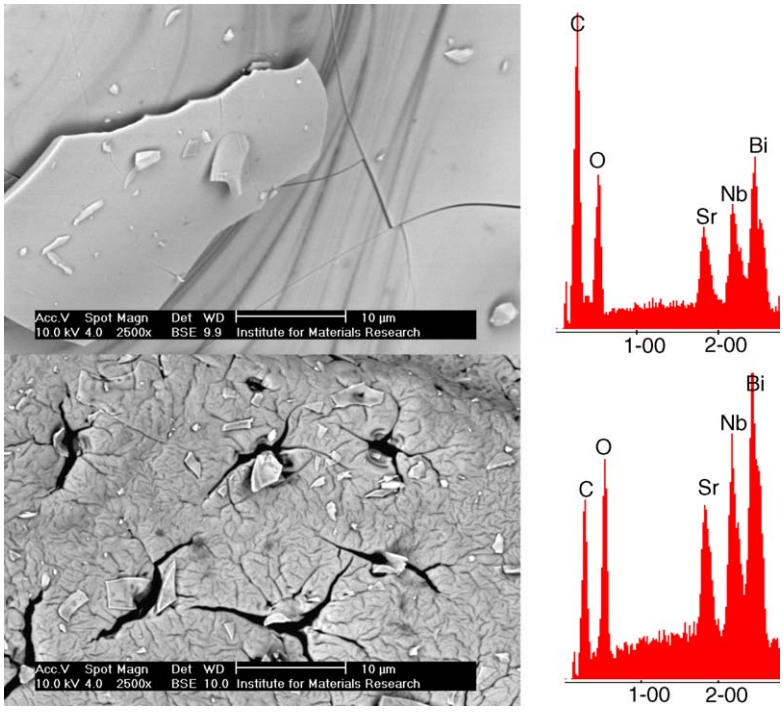

Fig. 2. SEM micrographs of the amorphous SBN precursor: (top) after thermal treatment at 400 °C, showing the typical appearance of a gel-glass; (bottom) after thermal treatment at 500 °C, showing a polycrystalline pellet after the nucleation of SBN-fluorite nanocrystallites and EDX results (right).

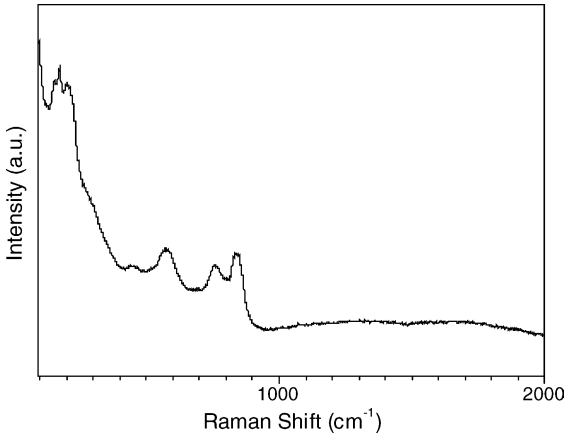

Fig. 3. The Raman scattering after thermal treatment at 550 °C shows only features of SBN-nanocrystallites and indicates the absence of amorphous carbon.

is readily detected by Raman. The absence of the typical features of amorphous carbon in the higher Raman shift region of Fig. 3 demonstrates that solid carbon is not present in the sample treated at 550 °C. The Raman features in Fig. 3 correspond only to SBN-nanocrystallites. The absence of luminescence effects and of amorphous carbon indicate that at 550 °C the combustion of the organic phase and also of the solid carbon resulting as byproduct of the combustion is complete.

Fig. 4 shows Raman spectra obtained from the sample treated at 550 °C taken at different points in the micro-mode over a reduced sample volume. The existence of two different spectra is clear. The characteristic Raman features of metastable fluorite-type SBN nanocrystallites, with a broad band centered at ∼750 cm^{-1}, are shown in the top graph in Fig. 4. Other Raman spectra (bottom graph in Fig. 4) show additional bands at ∼175, 205 and 840 cm^{-1}, characteristic of SBN with a Bi-layered perovskite structure. At this temperature treatment the Raman features corresponding to both structures appear together in many analyzed areas, but only those corresponding to SBN-fluorite appear in every spectrum. Therefore, we conclude that the sample treated at 550 °C is composed mainly by SBN-fluorite crystallites with scattered SBN-perovskite crystallites as a second phase. Considering that the approximate diameter of the analyzed area focussed by the exciting laser beam is ∼1 μm, both types of local order coexist closely and we must assume that nucleation of the stable SBN-perovskite occurs via the SBN-fluorite intermediate phase at this temperature. The SBN-fluorite is an intermediate phase where the three cations (Sr, Bi and Nb) occupy randomly the 8-coordination site typical of the fluorite structure. This more disordered structure is closer structurally to the amorphous than the stable Bi-layered perovskite structure and therefore forms as a metastable intermediate phase. The differences in the relative intensities of the Raman bands in the different spectra are caused by local inhomogeneities in the distribution of both phases.

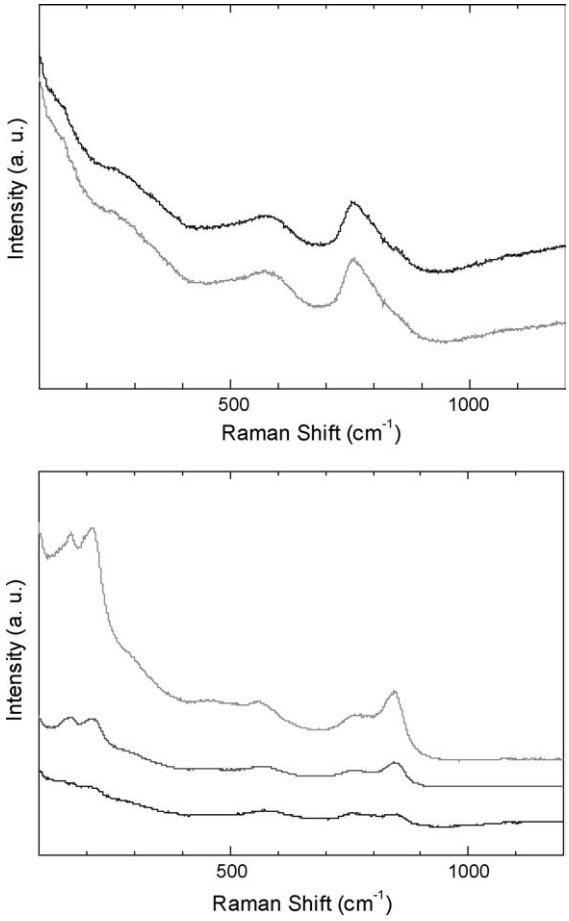

Fig. 4. Raman spectra taken at different points in the sample treated at 550 °C. Top: characteristic Raman spectra of fluorite-type SBN nanocrystallites. Bottom: other analyzed areas show additional features (main bands at ∼175, 205 and 840 cm^{-1}) characteristic of Bi-layered perovskite SBN.

We can observe the coexistence of the Raman bands corresponding to the fluorite and layered perovskite SBN crystallites also in the sample treated at 600 °C. Raman features of both phases are detected clearly in the macro mode over a wide analyzed area (Fig. 5). Both peaks are present in every spectra in this sample.

Raman scattering shows a great capability to detect changes in the local order involving significant variations in the anion–cation bond-forces, as it is the case here, with the new Raman bands associated to the perovskite. The XRD patterns at 550 and 600 °C (Fig. 1) do not detect the crystallization of any perovskite-SBN and show only wide peaks corresponding to SBN-fluorite. The absence of clear XRD features of the SBN-perovskite could be attributed to the small size of the crystallites. As the main peaks overlap, it is difficult to distinguish the smaller features characteristic of the SBN-perovskite pattern. It is of interest to compare the significant difference in crystallite sizes, calculated from XRD using the Scherer equation, between both SBN phases, and its evolution with temperature. Because the higher penetration of X-rays in the pellets, with sizes of several hun-

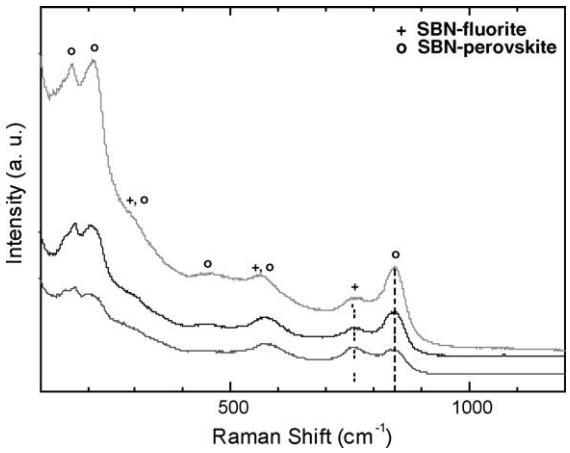

Fig. 5. Raman spectra in the sample treated at 600 °C. The peaks marked with vertical lines at ∼750 and 840 cm^{-1} corresponds to the main feature of SBN-fluorite and SBN–Bi-layered perovskite, respectively.

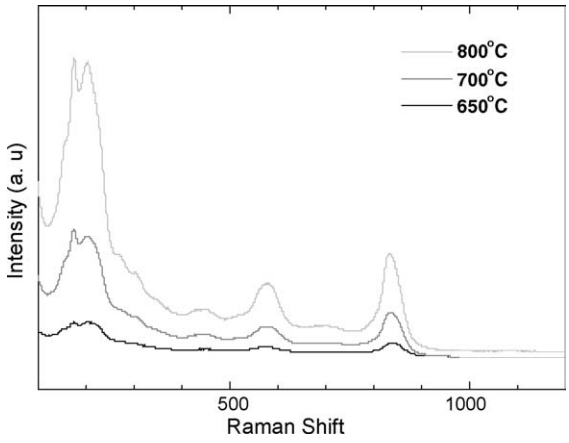

Fig. 6. Raman spectra after thermal treatment at 650, 700 and 800 °C, showing the typical spectra of perovskite-type SBN.

dred microns, the volume analyzed by Raman is predominantly at the surface compared to the XRD measurements. Further studies being carried out by TEM will clarify the crystallization process and if there is any enhanced crystallization at the surface which might cause the enhanced observation of the Bi-layered perovskite phase by Raman scattering.

At 650 °C and higher temperatures, 700 and 800 °C, Fig. 6, the disappearance of the band at ∼750 cm^{-1} clearly indicates the absence of fluorite-SBN.

3.3. Effect of the cooling rate

We have also studied the effect of the cooling rate on the Raman spectra. In the sample heated at 550 °C and slowly cooled, the Raman features characteristic of the SBN-perovskite phase (prominent bands at ∼170, 810 and 840 cm^{-1}) were clearly detected. However, in the rapidly cooled sample, only the features of SBN-fluorite—a characteristic spectrum with a broad main band at ∼750 cm^{-1}—were detected in all the analyzed areas. In the sample heated at 600 °C and rapidly cooled, the Raman features correspond clearly to the fluorite-type phase, while the slowly cooled sample shows prominent features of the layered perovskite-type phase. A high cooling rate resulted in the retention of more metastable phase with fluorite-type structure.

3.4. Assignment of Raman bands

To our knowledge, few studies have reported the Raman features of SBN.[16] Four wide Raman bands correspond to SBN-fluorite crystallites: three broad TO (A_1) phonons at ∼150, 250 and 570 cm^{-1} and a TO (E_g) phonon at ∼750 cm^{-1}. It is interesting to note the similarity of the spectra with the Raman features reported by Syam Prasad—ref.[16]—in a melt-quenched SBN-based glass with added $Li_2B_4O_7$. Although they attributed the observed modes to O–B–O vibrations, the spectra in fact clearly indicate the formation of fluorite SBN, as confirmed by their XRD and TEM measurements. In their samples, the fluorite peaks appeared shifted after quenching, but heating at 550 °C eliminated the shift.[16] The Bi-layered perovskite exhibits a more complex pattern, with up to 13 different bands identified in the Raman spectra obtained after thermal treatment at 800 °C (Table 1).

3.5. Evolution with temperature

The evolution of the most prominent features with temperature is shown in Fig. 7. There is a clear shifting on the Raman bands in the region of coexistence of both phases. This gradual shifting indicates the intimate mixing of both phases, so the local neighbourhood of the atoms in each phase is affected. The vibrational frequencies measured for the Bi-layered perovskite reach constant levels in the samples free

Table 1
Frequencies of the most prominent Raman features of the two phases at the different temperatures

T (°C)	Raman shift (cm^{-1})												
550	154	173	211	–	–	–		452		572		755	844
600	152	168	212	–	–	–	–	455	–	573	–	756	842
650	153	175	204	232	275	307	–	452	–	577	–	762	840
700	153	175	203	232	271	305	431	453	521	578	705	–	836
800	153	175	203	234	270	306	430	450	521	578	707	–	835

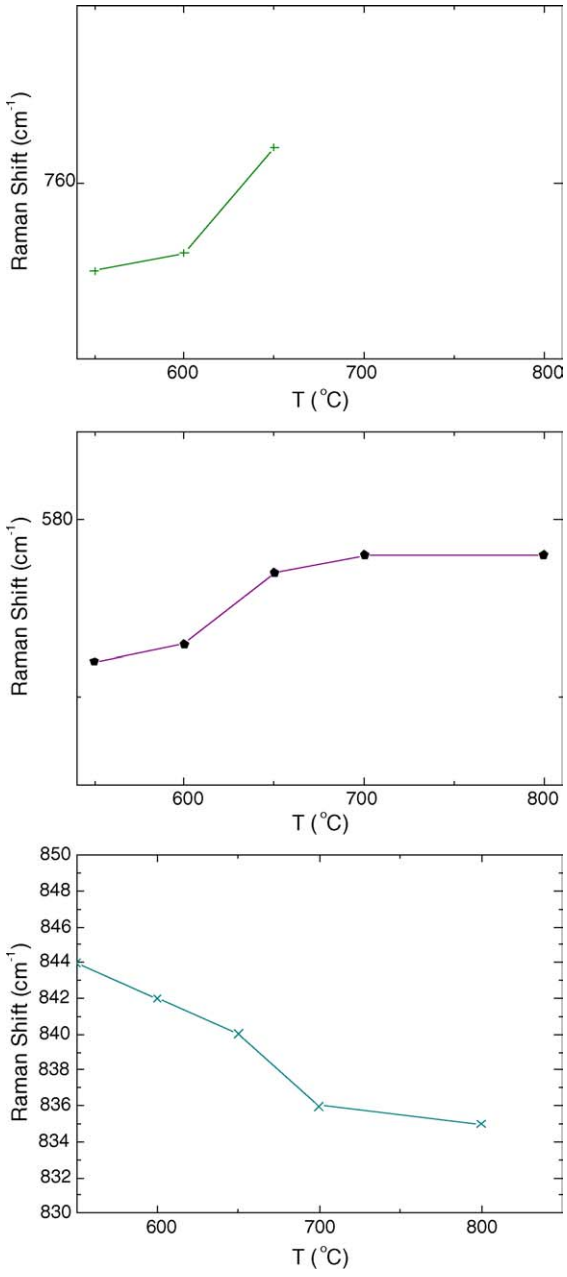

Fig. 7. Shifts on the vibrational frequencies observed in the region of coexistence of both phases.

of the intermediate and more disordered fluorite phase, above 650 °C. No peak shifting is observed between samples treated at 700 and 800 °C.

4. Conclusiones

We obtained single phase $SrBi_2Nb_2O_9$ nanocrystallites with fluorite-type structure below 500 °C, with Bi-layered perovskite at and above 650 °C, and mixtures of both between 550 and 650 °C, via the amorphous citrate route by controlling thermal treatment conditions.

Both phases show distinctive Raman features. The Raman study allows to determine clearly the thermal range of crystallization and the distribution of each phase in the mixtures. The Raman evolution with temperature showed band shifting in the region where the stable Bi-layered perovskite phase and the metastable fluorite phase coexist.

Acknowledgments

The study was carried out with financial support from the 'Ramón y Cajal' program from the Ministerio de Ciencia y Tecnología of Spain. The help of Dr. T. Jawhari with Raman measurements at the Serveis Cientificotecnics (SCT-UB, Barcelona) is gratefully acknowledged.

References

1. Durán-Martín, P., Castro, A., Millán, P. and Jiménez, B., Influence of the Bi-site subsditution on ferroelectricity of the Aurivillius compound $SrBi_2Nb_2O_9$. *J. Mater. Res.*, 1998, **13**, 2565.
2. Rodríguez, M. A., Boyle, T. J., Hernández, B. A., Buchheit, C. D. and Eatough, M. O., Formation of $SrBi_2Ta_2O_9$: Part II. Evidence of a bismuth-deficient pyrochlore phase. *J. Mater. Res.*, 1996, **11**, 2282.
3. Asai, T., Camargo, E. R., Kakihana, M. and Osada, M., A novel aqueous solution route for the low-temperature synthesis of $SrBi_2Nb_2O_9$ by the use of water soluble Bi and Nb complexes. *J. Alloys Compounds*, 2000, **309**, 113.
4. Zanetti, S. M., Santiago, E. I., Bulhões, Varela, J. A., Leite, E. R. and Longo, E., Preparation and characterization of nanosized $SrBi_2Nb_2O_9$ powder by the combustion synthesis. *Mater. Lett.*, 2003, **57**, 2812.
5. Zanetti, S. M., Leite, E. R., Longo, E. and Varela, J. A., $SrBi_2Nb_2O_9$ thin films deposited by dip coating using aqueous solution. *J. Eur. Ceram. Soc.*, 1999, **19**, 1409.
6. Zanetti, S. M., Vasconcelos, J. S., Vasconcelos, N. S. L. S., Leite, E. R., Longo, E. and Varela, J. A., $SrBi_2Nb_2O_9$ thin films crystallized using a low power microwave oven. *J. Eur. Ceram. Soc.*, 2004, **24**, 1597.
7. Yi, J. H., Thomas, P., Manier, M., Mercurio, J. P., Jauberteau, I. and Guinebretiere, R., SrBi2Nb2O9 ferroelectric powders and thin films prepared by sol–gel. *J. Sol-Gel Sci. Technol.*, 1998, **13**, 885.
8. Yang, H.-M., Luo, J.-S. and Lin, W.-T., In situ growth of fatigue-free $SrBi_2Nb_2O_9$ by pulsed laser ablation. *J. Mater. Res.*, 1997, **12**, 1145.
9. Boyle, T. J., Buchheit, C. D., Rodríguez, M. A., Al-Shareef, H. N., Hernández, B., Scott, J. W. *et al.*, Formation of $SrBi_2Ta_2O_9$: Part I. Synthesis and characterization of a novel sol–gel solution for production of ferroelectric $SrBi_2Ta_2O_9$ thin films. *J. Mater. Res.*, 1996, **11**, 2272.
10. Ito, Y., Yoshikubo, M., Yokoyama, S., Matsunaga, H., Atsuki, T., Yonezawa, T. *et al.*, New low-temperature processing of sol–gel $SrBi_2Ta_2O_9$ thin films. *Jpn. J. Appl. Phys.*, 1996, **35**, 4925.
11. Nelis, D., Van Werde, K., Mondelaers, Vanhoyland, G. D., Van Bael, M. K., Mullens, J. *et al.*, Synthesis of $SrBi_2Ta_2O_9$ by means of a soluble Ta(V) precursor. *J. Eur. Ceram. Soc.*, 2001, **24**, 2047.
12. Nelis, D., Van Bael, M. K., Van den Rul, H., Mullens, J., Van Poucke, L. C., Vanhoyland, G. *et al.*, Ferroelectric $SrBi_2Nb_2O_9$ thin films by aqueous chemical solution deposition. *Integr. Ferroelectr.*, 2002, **45**, 205.
13. Nelis, D., Van Bael, M. K., Mullens, J. and Van Poucke, L. C., Aqueous solution gel synthesis of strontium bismuth niobate ($SrBi_2Nb_2O_9$). *J. Sol–Gel Sci. Technol.*, 2003, **26**, 1125.

14. Narendar, Y. and Messing, G. L., Synthesis, decomposition and crystallization characteristic of peroxo-citrato-niobium: an aqueous niobium precursor. *Chem. Mater.*, 1997, **9**, 580.
15. Hardy, A., Mondelaers, D., Van Bael, M. K., Mullens, J., Van Poucke, L. C., Vanhoyland, G. *et al.*, Synthesis of $(Bi,La)_2Ti_3O_{12}$ by a new aqueous solution gel-route. *J. Eur. Ceram. Soc.*, 2004, **24**, 905.
16. Syam Prasad, N. and Varma, K. B. R., Nanocrystallization of $SrBi_2Nb_2O_9$ from glasses in the system $Li_2B_4O_7$–SrO–Bi_2O_3 –Nb_2O_5. *Mater. Sci. Eng.*, 2002, **B90**, 246.